Algal bloom monitoring in Koka Reservoir, Ethiopia: Application of satellite remote sensing algorithms

Eden Eritrea[1], Yoshihiko Inagaki, Rodgers Makwinja

1 Addis Ababa University

Funding: No specific funding was received for this work.

Potential competing interests: No potential competing interests to declare.

Abstract

Koka Reservoir in Ethiopia, which serves as an essential water source for local inhabitants, has faced severe toxic cyanobacteria blooms. A conventional technique has been employed to monitor the trend. Though this technique has been proven accurate, it has been expensive and laborious. Hence, a satellite remote sensing technique is proposed to offset these challenges. The main objective of this paper is to explore two satellite-derived indices, which involved cross-validation of the floating algal index (FAI) derived from Sentinel-2 MSI and Landsat-8 OLI imagery. We further investigated the link between the FAI and normalized difference chlorophyll index (NDCI) using Sentinel-2 MSI. The findings showed that FAI values derived from MSI imagery were slightly higher than those derived from OLI imagery. A strong positive linear regression coefficient (R^2 = 0.82), indicated that the FAI algorithm is a sensor-insensitive-suggesting it could be used for algal bloom monitoring in Koka Reservoir.

Eden Eritrea[a*], **Yoshihiko Inagaki**[a, b], and **Rodgers Makwinja**[c,d]

[a]Africa Centre of Excellence for Water Management, College of Natural and Computational Sciences, Addis Ababa University, P. O. Box 1176, Addis Ababa, Ethiopia

[b]Department of Civil and Environmental Engineering, Waseda University, Shinjuku, Tokyo 169-8555, Japan

[c]Ministry of Forestry and Natural Resources, Fisheries Department, Senga Bay Fisheries Research Center, P. O. Box 316, Salima, Malawi

[d]WorldFish Malawi Office Garden Court Office Park, Area 11, Office block 3 P. O. Box 30294. Capital City, Lilongwe, Malawi

[*]The author to whom correspondence should be addressed:eden.eritres@aau.edu.et

Keywords: Algal bloom monitoring; Floating algal index; Sentinel-2 MSI; Landsat-8 OLI imagery; Koka Reservoir.

Introduction

The spread of harmful algal blooms in water bodies is now a significant concern for the entire world (Trottet et al. 2021). It is driven by increased domestic and commercial sewage discharges, excessive use of fertilizers and manure in agriculture, and eutrophication of surface waters (Haque, 2021). Algal blooms are typically associated with severe depletion of oxygen, drastically reducing water transparency, and the formation of toxins- threatening aquatic and terrestrial organisms and human health (Major et al., 2018). Numerous cyanobacterial toxins have been linked to acute and potentially chronic public health issues and the lethal poisoning of domestic and aquatic animals. Consuming seafood, such as fish raised in areas where harmful algal blooms exist, poses the same public health risk as cyanobacterial toxins (Tilahun & Kifle, 2019). Currently, the Koka Reservoir, the subject of this study, is in the worst condition, with *Microcystis aeruginosa* dominating the cyanobacterial assemblage. The number of total microcystins (MCs) has significantly exceeded the WHO-permitted standard (1µg/L) (Tilahun et al., 2019). A situation that requires urgent attention and regular monitoring of the reservoir.

Over the past decades, a conventional water quality monitoring technique has been employed in the Koka Reservoir. Though this technique has been proven accurate, it has failed to consider the spatial variability of water quality parameters in the reservoir. Several chlorophyll-a algorithms have been demonstrated to perform well with satellite imagery to estimate concentrations in turbid inland water bodies. These include a semi-analytical NIR-Red band algorithm for MERIS (Gons et al., 2005), Cyanobacteria Index(Wynne et al., 2008), 708/665 empirical band ratio (Gilerson et al., 2010), Maximum Peak Height (Matthews et al., 2012) and Normalized Difference Chlorophyll Index (NDCI; Mishra and Mishra, 2012). However, these algorithms have not been applied extensively to Ethiopian lakes. Sentinel-2, a land monitoring constellation of two satellites launched in 2015 and 2017, offers enhanced spatial (10-60 m) and temporal resolution (5 days) (Soomets et al., 2020). They are perfect for monitoring small to medium-sized lakes and reservoirs. They also provide excellent coverage of water constituents. The thermal infrared sensors aboard the Landsat satellites, operational since 1984, can also perform retrospective analysis and monitor the surface temperature of small to medium-sized lakes and reservoirs every two weeks (Sharaf, 2021). The floating Algal Index (FAI), also initially developed by Hu (2009) for the Moderate Resolution Imaging Spectrometer (MODIS), has been highly recommended for monitoring surface oil slicks, algal blooms, and coastal water quality.

The FAI is calculated by subtracting a reflectance value in the near-infrared (NIR) from the baseline reflectance in the NIR band that is derived from a linear interpolation between the red and short-wave infrared (SWIR) bands. The underlying idea of this index is that floating algae have higher reflectance in NIR than other wavelengths such that they can be easily distinguished from water. This index is characterized by the robustness to environmental and observing conditions (Hu, 2009). Sentinel-2 MSI and Landsat-8 OLI are equipped with the above three necessary bands to obtain FAI. To effectively estimate chl-a in turbid waters, the Normalized Difference Chlorophyll Index (NDCI) has also been proposed by Mishra and Mishra (2012) for the Medium Resolution Imaging Spectrometer (MERIS) sensors. These researchers established a strong polynomial relationship between NDCI values and in-situ measured chl-a. The index is calculated using two bands, of which the central wavelengths are 708 nm and 665 nm, respectively. The two wavelengths represent the reflectance

peak and absorption feature of chl-a. Page et al. (2018) slightly modified this algorithm for Sentinel-2 MSI and exploited the 704 nm wavelength instead of 708 nm.

Since the band centered at 704 nm is lacking in the OLI sensor, it is impossible to calculate an NDCI value and a chl-a concentration directly. However, Page et al. (2018) demonstrated that the relationship between processed Sentinel 2 MSI-derived FAI and NDCI (denoted hereafter as FAI_{MSI} and $NDCI_{MSI}$) could be exploited to derive NDCI values and subsequent chl-a concentrations, even when the OLI sensor is used. In this study, the application of the FAI technique is essential because the Sentinel-2 MSI imagery for Lake Koka is available in Google Earth Engine (GEE) after December 2018, while the Landsat-8 OLI has been available since May 2013. The field data from 2013 to 2017 is also available. GEE is a robust cloud-based spatial analytical tool, and users can access various image collections. GEE provides Level-2 products for OLI and MSI images and can be used without atmospheric correction.

Therefore, the main objective of this study is to explore two satellite-derived indices, which involved cross-validation of the FAI derived from Sentinel-2 MSI and Landsat-8 OLI imagery, as well as investigating the link between the FAI and NDCI using Sentinel-2 MSI to demonstrate temporal and spatial heterogeneity of optical characteristics in the Koka Reservoir, which reflects phytoplankton dynamics in the water body. We further attempted to understand chl-a distributions in the whole part of the reservoir in different seasons, using NDCI that can be used as an indirect index to measure chl-a abundance. The created maps were associated with variations in land surface temperature and precipitation in this region.

Methods

Description of the study

The Koka reservoir (Fig 1), also known as Lake Galilea, was created in 1960 by constructing the Koka Dam across the Awash River to generate hydroelectricity. It is located in the Misraq Shewa Zone of the Oromia Region, about 90 kilometers south of Ethiopia's capital city, Addis Ababa, at 8°45′ N and 39°15′ E. The Koka reservoir is fed by two rivers, the Awash (primary) and the Mojo (minor), which flow into it from the west (Getnet et al., 2021). Koka reservoir is used not only for generating electricity but also it is known for its domestic water supply, commercial fish farming, recreation, and irrigation. The reservoir is also known for tourism (Fasil et al., 2011).

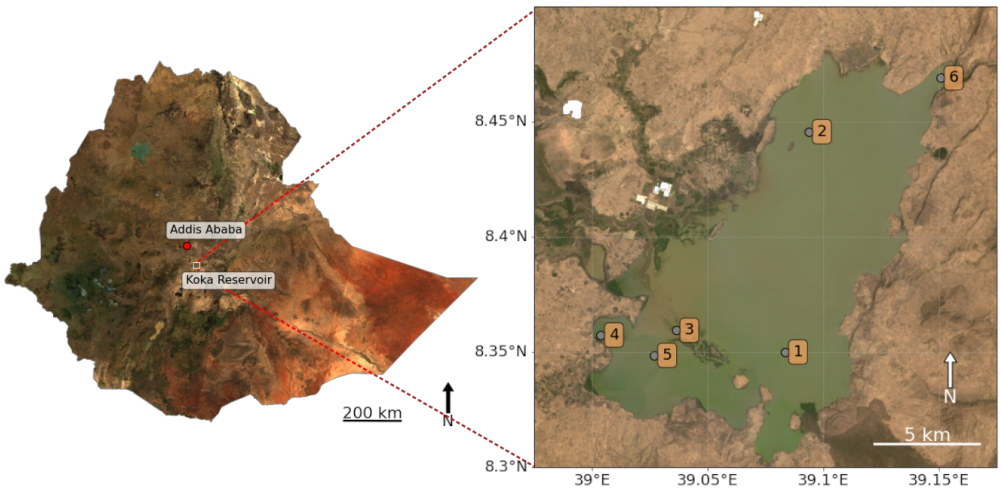

Figure 1. Map of Koka Reservoir with sampling sites

Data collection approach

We first exploited Joint Research Center (JRC) Global Surface Water Occurrence data, version 1.3, to remove land areas from the lake boundary. The reflectance from land surfaces was avoided for the analysis. We further adopted a technique that Donchyts et al. (2016) proposed, including Normalized Difference Water Index, the Canny edge filter, and Otsu thresholding. After delineating water areas, we assessed the similarity between FAI_{MSI} and Landsat-8 OLI processed FAI images (FAI_{OLI}) in randomly generated points over the entire lake. Images of two dates (i.e., December 15, 2018, October 31, 2019) were subject to this analysis since the overpass times of the two satellites were almost coincident (within 20 min). After that, we examined the relationship between FAI_{MSI} and $NDCI_{MSI}$ in other randomly generated points using 12 cloud-free MSI images throughout the year 2019 (i.e., January 9 and 14, February 13, March 15, April 14 and 29, May 4 and 19, June 13, September 1, October 21, and November 15). Forty random points were generated per image, and 400 out of 480 pairs of FAI and NDCI values were retrieved and used to establish the correlation. From January to April, a part of the lake dried up, and some water areas in the south were almost isolated from the rest. We split the lake into two parts accordingly and generated random points to investigate different behaviors in these two parts. The resulting regression equation between FAI_{Sen2A} and $NDCI_{Sen2A}$ was further evaluated to compare FAI_{OLI} with $NDCI_{MSI}$ at four different times (i.e., April 8, June 27, September 15, December 4, 2020), when both satellite overpasses were coincident. Meanwhile, the relationship between FAI_{OLI} and in-situ chl-a concentrations was examined using field sampling data obtained at three offshore locations (i.e., sites No. 1-3) from 2013 to 2016 (the total number of data points was 27) and three other different locations (i.e., sites No. 4-6) on May to August 2017 (the total number of data points was 12). Figure 1 shows the locations of sampling points covered in this study, of which more detailed information is summarized in Table 1.

Table 1. Sampling site information

Site id	Coordinates	Sampling months	References
1	8.350°N, 39.083°E	August, December 2013, February to April 2014	Major (2016)
2	8.446°N, 39.094°E	March, April, May, October, November 2015 January 2016	Zewde et al. (2018)
3	8.359°N, 39.036°E	May 2015 to April 2016 (except September 2015)	Tilahun and Kifle (2019)
4	8.357°N, 39.004°E	May to August, 2017	Aynalem (2018)
5	8.349°N, 39.027°E		
6	8.469°N, 39.151°E		

Finally, mappings of NDCI values using MSI imagery were created over the entire lake in three different seasons (dry, minor rainy and heavy rainy) in 2021: February 2, May 18 and September 10 as representative data for the three seasons. We used MODIS-derived land surface temperature data for auxiliary climate-related data, an average-8-day composite data in a 1200 × 1200-kilometre grid. The central point of the lake (8.393°N, 39.090°E) and a location near the west shoreline (8.420°N, 39.014°E) were chosen as monitoring points for MODIS imagery. Additionally, we obtained precipitation data via Global Rainfall Map (GSMaP_MVK) by JAXA Global Rainfall Watch (produced and distributed by the Earth Observation Research Center, Japan Aerospace Exploration Agency).

Results

The FAI values derived from MSI imagery were slightly higher than those derived from OLI imagery, but a strong positive linear correlation (R^2 = 0.82) was observed between FAI_{Sen2} and FAI_{OLI} (Figure 2a). This indicates that the FAI algorithm is rather sensor-insensitive. A relationship between FAI_{MSI} and $NDCI_{MSI}$ is displayed in Figure 2b.

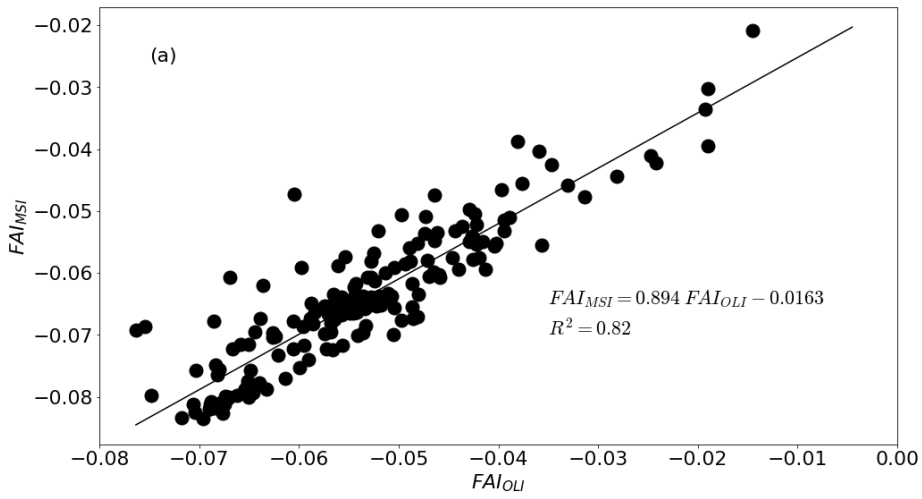

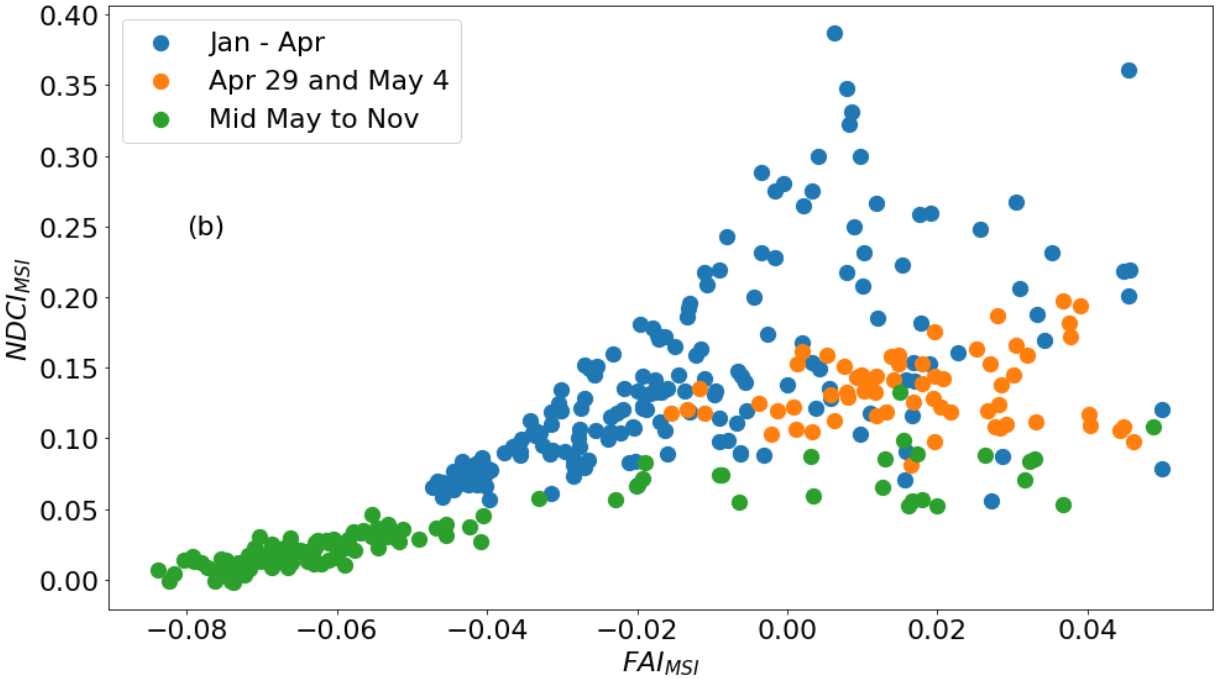

Figure 2. (a) Relationship between MSI-derived FAI vs OLI-derived FAI, and *(b) relationship between MSI-derived FAI vs NDCI. Note: The former was based on images of 2 dates when both satellite overpasses were coincident on December 15, 2018, and October 21, 2019. One hundred random points were generated over the entire lake for each image, and 192 out of 200 pairs were retrieved and displayed. For the latter, 12 cloud-free MSI images throughout the year 2019 (i.e., January 9 and 14, February 13, March 15, April 14 and 29, May 4 and 19, June 13, September 1, October 21, and November 15) were obtained. Fourth random points were generated per image, and 400 out of 480 pairs of FAI and NDCI values were retrieved and used to establish the correlation.*

The plot colors were changed depending on the times: (i) January to April, (ii) April 29 and May 4, and (iii) middle May to November. The FAI values lower than -0.05 consist of the only dataset from the middle of May to November, and even in higher FAI values than -0.05, NDCI values were consistently lower for this dataset. Plots of the dataset from April 29 and May 4 were located in the middle of the other two datasets but still close to the dataset from the middle of May to November. However, the dataset from January to April exhibited higher NDCI values, even with lower FAI values. We further investigated data for January to April. Scatter plots for the north and south parts are presented in Figure 3.

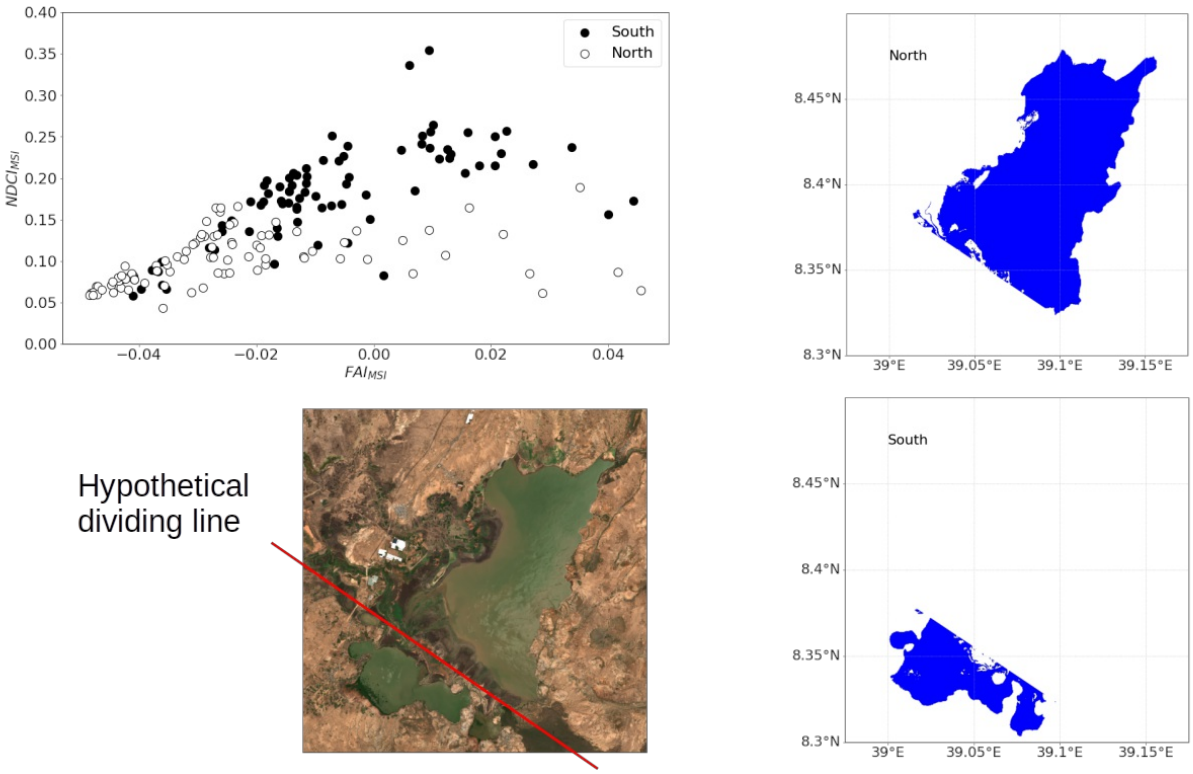

Figure 3. Scatter plots of MSI-derived FAI vs NDCI for January to April. The entire lake was split into two parts, namely the north and south, of which the red line represented the boundary

Plots from the south part exhibit higher NDCI values compared with those from the north parts. To derive a relationship between FAI_{MSI} and $NDCI_{MSI}$, we decided to separate data from the south part from the January to April data, while data from the north part were combined with data from May to November. In Figures, 4a and b, the resulting linear regressions were shown, and the regression equations were $NDCI_{MSI} = 1.13\ FAI_{MSI} + 0.106$ ($R^2 = 0.66$), and $NDCI_{MSI} = 2.33\ FAI_{MSI} + 0.215$ ($R^2 = 0.43$), respectively. We further confirmed the two patterns of FAI vs NDCI with a dataset obtained at four different times (i.e., April 8, June 27, September 15, and December 4, 2020) when both satellite overpasses were coincident. Again, we observed in Figure 4c that in April and December, NDCI values were consistently higher than those in June and September. Next, we looked into a relationship between FAI_{OLI} vs in-situ chl-a. In-situ data were obtained at three offshore sampling locations (sites No. 1 to 3) from 2013 to 2016 (N=27) and obtained at sites No. 4 to 6 from May to August 2017 (N=12).

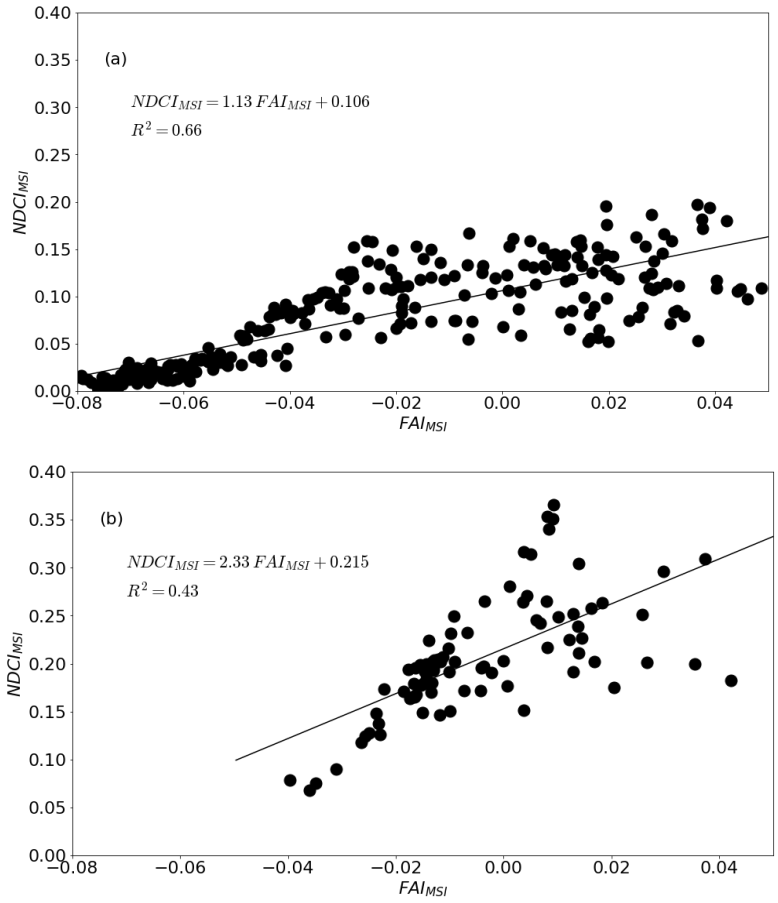

Figure 4. (a) Resulting relationship between MSI-derived FAI vs NDCI for (a) January to April data of the north part as well as May to November data of the whole part, (b) January to April data of the south part

As shown in Figure 5, (a) and (b), data from site No.2 were well fitted to the previously proposed equations (Mishra and Mishra, 2012 and Makwinja et al. (2022); however, data from site No.1 and No.3 were consistently higher or lower than the solid or dashed lines. We acknowledged that sampling dates were unknown exactly, except for months, and there might be a possibility that sampling water contained higher chl-a. However, based on the stability of FAI values in about 20 days, the Lake Koka waters appeared to be not very variable within this range, so we suspect that chl-a concentrations in site No.1 were too high. Also, there were typically macrophytes near site No.3, which might have caused apparent high FDI values.

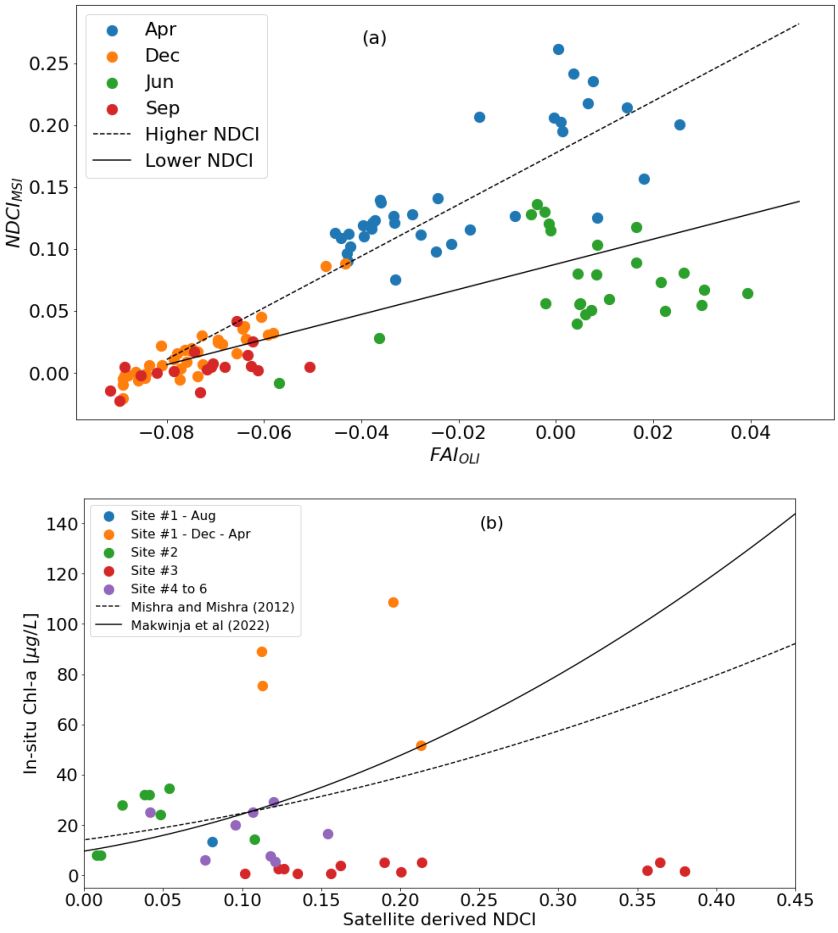

Figure 5. (a) Comparisons of MSI-derived NDCI to OLI-derived FDI at four different times (i.e., April 8, June 27, September 15, December 4, 2020), when both satellite overpasses were coincident, (b) the relationship between OLI-derived NDCI vs in-situ chl-a obtained at three offshore sampling locations (site No. 1 to 3) in 2013 to 2016 (N=27) and obtained at sites No. 4 to 6 in May to August 2017 (N=8).

OLI-derived NDCI and the higher and lower NDCI lines in Figure 5(a) were obtained from equations presented in Figures 2 and 3. FAI_{OLI} was first converted to FAI_{MSI}, and then NDCI was calculated based on the two different regression equations. The error analysis was conducted for April and June datasets in Figure 5(a). The mean absolute percentage errors for those datasets were 20.0 and 36.2%, respectively.

Figure 6 shows the $NDCI_{MSI}$ distribution maps for the entire lake in three different seasons, which are dry, minor rainy, and heavy rain. Considering that an NDCI value is positively correlated with a chl-a concentration as demonstrated by previous studies, even though there are no established equations to estimate chl-a obtained in this study, we can understand a spatio-temporal variation of NDCI distribution maps as a proxy for chl-a concentration maps. In a dry season, the south part exhibited higher values, while the rest showed relatively low values, and the distribution was homogeneous (Figure 6a).

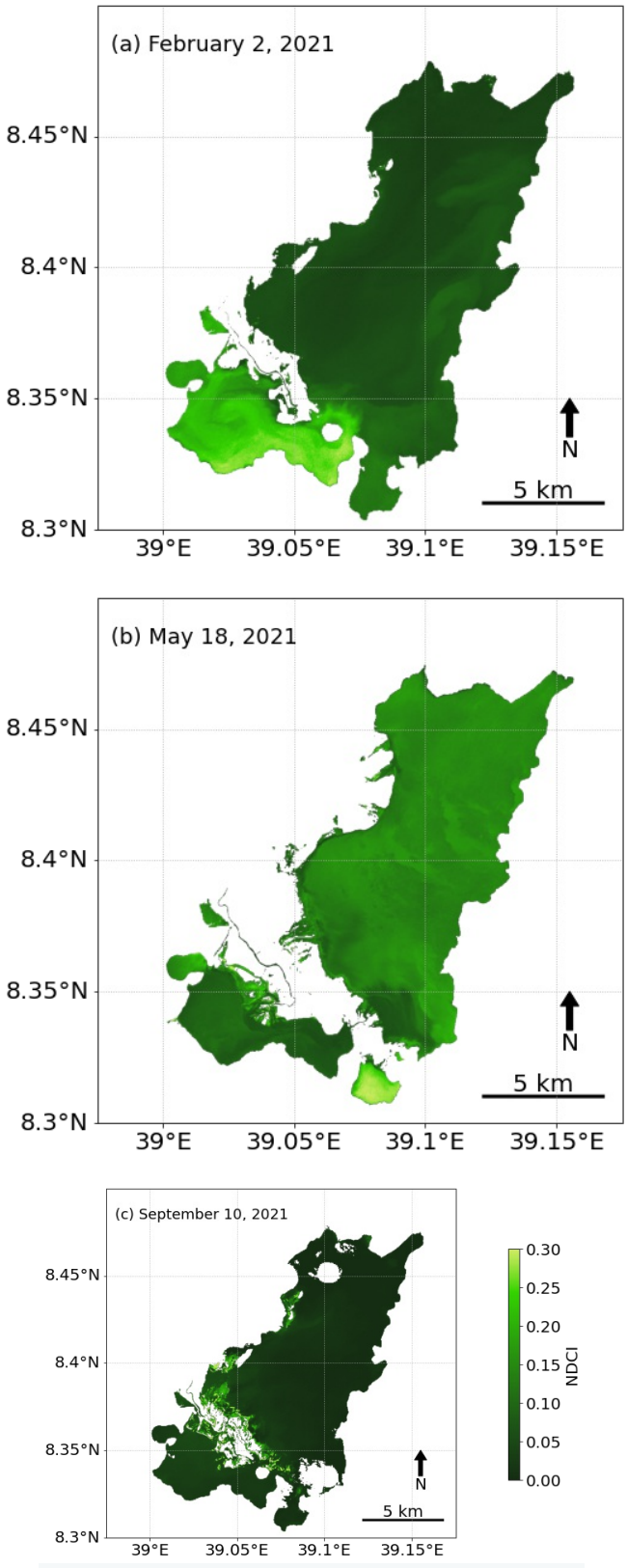

Figure 6. NDCI mapping for Lake Koka at three different seasons (minor rainy, heavy rainy, and dry): (a) February 2, 2021; (b) May 18, 2021; (c) September 10, 2021.

On the contrary, in a minor rainy season, the northern part exhibited higher values, compared with the south, except for the isolated small part in the south. It turned out that the NDCI values got lower almost entirely in a heavy rainy season. As can be seen in Figure 7, surface water temperatures were stable in a range of 18 to 25℃ for the entire year; however, surface land temperatures tended to be higher, particularly in the first half of the year, peaking at higher than 45℃ in May, and dropped to less than 30℃ when the heavy rainy season started in June. After that, the surface temperature gradually incremented toward the end of the year.

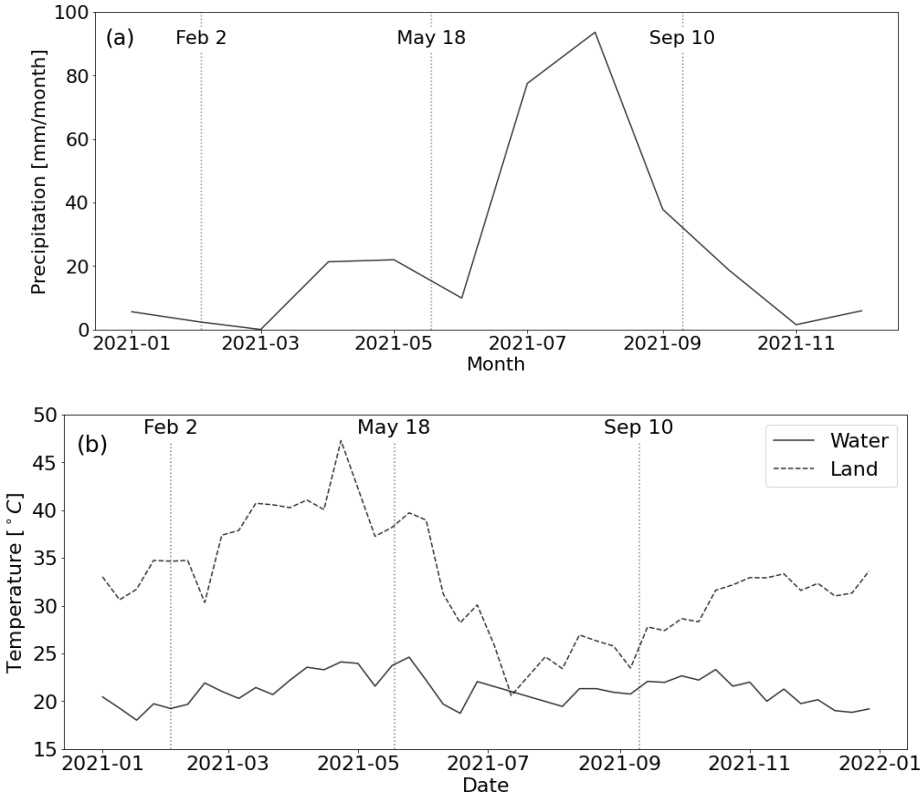

Figure 7. (a) Precipitation and (b) surface temperature data (water and land) in the Lake Koka region in the whole year of 2021. The central point of the lake (8.393°N, 39.090°E) and a location near the west shoreline (8.420°N, 39.014°E) were chosen as representative monitoring points.

Discussion

Financial and institutional constraints hinder in situ water quality data availability in lakes in remote areas such as Koka Reservoir. Additionally, in situ monitoring has limited spatial and temporal coverage, making it difficult to obtain information on water quality dynamics across the lake. The introduction of remote sensing applications overcomes the drawbacks that traditional field monitoring methods have and would open new perspectives for lake monitoring (Bouffard et al., 2018). This study demonstrated the first application of satellite image analysis to Koka Reservoir to facilitate an understanding of phytoplankton dynamics and to monitor water resources with a fine-scale spatial variation. As Willén et al. (2011) reported, Koka Reservoir has suffered from recurrent blooms of *Microcystis aeruginosa*, the dominant species

among the cyanobacterial assemblage. Blue-green surface scum is often observed on the water surface. This was thought to be a good situation where the utility of FAI was proven. This study, however, showed that relying solely on FAI was not acceptable since there were two patterns between FAI vs NDCI relationships, as demonstrated in Figure 2 (b), unlike the single relationship observed in the literature (Page et al., 2018).

This study further revealed the spatial and seasonal heterogeneity of optical characteristics of water in Koka Reservoir. Koka Reservoir is divided into two parts in half a year in terms of optical properties (see Figure 3). In addition, there are three distinct seasons in the region where Koka Reservoir is located: dry, minor rainy and heavy rainy seasons. The relationship between FAI and NDCI revealed that we could group datasets of the nearly whole year (January to November) into two subsets: (i) January to April data of the north part plus May to November data, (ii) January to April data of the south part. This observation could not have been achieved without satellite data and a novel finding for Koka Reservoir. Agricultural lands are considered a significant source of nutrient inputs for Koka Reservoir. Rapid population growth and intensive agriculture practices, especially in the Awash catchment, have accelerated soil erosion. The surface runoff in the catchment during a heavy rainy season (from mid-June to mid-September) causes the river to transport sediment and nutrient into the Koka Reservoir (Tilahun et al., 2019). The accumulated nutrients could lead to cyanobacteria proliferation observed during other months (i.e., dry and minor rainy seasons) (Major et al., 2018). These phenomena were detected with NDCI mappings, as shown in Figure 6.

Interestingly, our results showed that in a dry season, high activity of phytoplankton in the Koka Reservoir was mainly distributed in the southern part; however, this distribution was shifted to the northern part (a vast part of the reservoir) in a minor-rainy season. As another nutrient input to Koka Reservoir in a dry season, Tilahun and Kifle (2021) studied atmospheric sources and found that this was indeed associated with high concentration levels of ammonia. They suspected that the origin was direct emission from fertilized agricultural lands and animal wastes produced from livestock. Ammonia is favourable for cyanobacteria since the assimilation requires less energy (Tilahun and Kifle, 2021). Tilahun and Kifle (2019) reported that the observed low level of nitrogen and soluble reactive phosphorus in 2015 could probably be related to a reduction of nutrient inputs delivered through rivers due to El Niño induced drought in Ethiopia. The low concentrations of nitrogen and phosphorus may also have resulted from active denitrification processes and adsorption to the existing abundant silt due to the intense mixing of the shallow water column, respectively (Zewde et al., 2018). During this period, the proliferation of diazotrophic cyanobacteria was observed, as they have a tolerance to severely limited nitrogen conditions and can fix nitrogen gas. However, phosphorus can be replenished through an internal cycle from the sediment pool (Tilahun and Kifle, 2019). When the sediment condition is anoxic, phosphorus retention is low, making the lake system more vulnerable to external inputs. This means that long-term increases in phytoplankton could be induced due to a rise in phosphorus loads from the watershed, as observed in another African lake, Lake Malawi (Li et al., 2018). The southern portion of Koka Reservoir exhibited particularly in a dry season consistent higher NDCI values, which indicate phytoplankton activities. This part is most affected by the impacts of land use in the Awash catchment. The proper management to mitigate nutrient load from the catchment will be required to prevent further degradation of the reservoir's water quality.

According to Tilahun et al. (2019), the concentration level of total microcystins (MCs) reached 45–54 µg/L, far beyond the

permissible level (1 µg/L) set by WHO. They observed exceptionally high concentrations of MC variants in May; however, the concentrations decreased from October to February, and those of extra-cellular MC variants were below the detection limit. They suggested that the intense solar radiation and high water temperature induced photolysis and bio-degradation of the extra-cellular toxins, leading to low levels of those toxins in most months throughout the year. However, sparse monitoring data make it difficult to accurately assess the whole situation, as point estimates typically do not represent the entire part of the reservoir. Since there is no practical method to estimate the toxin from satellite imagery directly, we still need to rely on chl-a concentrations or subsequently estimated cyanobacteria cell counts. The plausible range of the alert level for toxic cyanobacteria species is between 12 and 25 µg/L set by WHO (Matthews et al., 2012). To mitigate blooms and their toxins, understanding the link between environmental variables and spatio-temporal dynamics of cyanobacteria is crucial to managing Koka Reservoir effectively. Those variables include physicochemical, biological and climatological factors (e.g., water temperature, pH, nutrient availability, transparency, and solar radiation) (Tilahun and Kifle, 2019). Considering the cyanobacteria's ability to adjust their vertical position with its gas vacuoles, conditions leading to the dominance of cyanobacteria have been well studied in the literature (Major et al., 2018): low light, high temperature, and low euphotic depth to mixing depth ratio. (Paerl, 2014) reported that cyanobacteria growth is inhibited when water temperature exceeds 35°C. According to MODIS-derived water surface temperature, water in Koka Reservoir appears to be stable in the range of 20-25°C, which means that cyanobacteria growth is less likely to be diminished due to this factor. Dilution of the reservoir water due to precipitation contributes to mitigating cyanobacteria bloom(Coffer et al., 2020). In fact, as shown in Figure 6 (c), phytoplankton activity was apparently suppressed across the entire part during a heavy rainy season. The solar radiation in this region is intense, except for a heavy rainy season, based on MODIS-derived land surface temperature [see Figure 7(b)]. As noted earlier, cyanobacteria have a unique capacity to adjust their positions with buoyancy. Under strong sunlight, they move lower in the water column, which may cause an under-representation of satellite-derived indices(Coffer et al., 2020). The discrepancy between field observations (particularly ones obtained in site No.1) and satellite data observed in Figure 5 (b) can be explained by this situation.

As Koka Reservoir serves as an essential water resource for people living nearby, the remote sensing application could be extended to an early warning system to let the public know about the possible occurrence of blooms. It is beneficial for local inhabitants to understand where and when algal bloom occurs at a specific point of interest. However, we need to note that satellite remote sensing has some limitations. Satellite images are unavailable when the water surface is covered with clouds, typically during a rainy season (Sawtell et al., 2019). Another limitation is that the satellite sensor is unable to detect portions of water in the depth direction, which could fail to capture the stratified structure of phytoplankton distributions in the water column. Also, in areas very close to the shore, water is optically shallow and could induce false signals from bottom reflectance, which could be misinterpreted as phytoplankton (Coffer et al., 2020). Some of these limitations can be resolved with the integration of in-situ and remote sensing data with numerical simulations (Bouffard et al., 2018).

Conclusion

An effective way to complement time-consuming field monitoring activities is through satellite remote sensing. There has been a demand for remote sensing-based water quality monitoring systems because of the rise in the frequency of algae blooms and the global degradation of water, including Koka Reservoir. This study was successfully completed using two operational satellite sensors on the Koka reservoir. Cross-validation of the FAI derived from Sentinel-2 MSI and Landsat-8 OLI imagery was also performed, and the results demonstrated that the FAI algorithm is relatively sensor-insensitive because FAI derived from MSI imagery were slightly higher than those derived from OLI imagery but had a strong positive linear correlation. Furthermore, based on the image generated in this study, the Koka reservoir appears to be divided into two parts in half a year by its optical properties, revealing the spatial and seasonal heterogeneity of water's optical characteristics. For nearly a year, arranging and grouping the reservoir datasets was possible based on the FAI-NDCL relationship results. Additionally, NDCL mapping revealed a high activity of phytoplankton in the Koka reservoir, first in the southern part and then spreading to the north during a minor rainy season. In general, the overall results from the Sentinel-2 and Landsat-8 platforms, combined with more systematic in-situ sampling, will play a considerable role in fully understanding the phytoplankton community in Koka Reservoir, as well as pave the way for authorities to develop concrete monitoring systems based on detailed information and spatially variable data generated by both satellite remote sensing algorithms and filed data.

References

- Bouffard, D., Kiefer, I., Wüest, A., Wunderle, S., & Odermatt, D. (2018). Are surface temperature and chlorophyll in a large deep lake related? An analysis based on satellite observations in synergy with hydrodynamic modelling and in-situ data. *Remote Sensing of Environment*, *209*(August 2017), 510–523. https://doi.org/10.1016/j.rse.2018.02.056
- Coffer, M. M., Schaeffer, B. A., Darling, J. A., Urquhart, E. A., & Salls, W. B. (2020). Quantifying national and regional cyanobacterial occurrence in US lakes using satellite remote sensing. *Ecological Indicators*, *111*(September 2019). https://doi.org/10.1016/j.ecolind.2019.105976
- Donchyts, G., Schellekens, J., Winsemius, H., Eisemann, E., Van de Giesen, N., 2016. A30 m resolution surface water mask including estimation of positional and thematic differences using Landsat 8, SRTM and OpenStreetMap: A case study in the Murray-Darling Basin, Australia. Remote Sensing 8, 386
- Fasil, D., Gashaw, T., & Aschalew, T. (2011). Some limnological aspects of Koka reservoir, a shallow tropical artificial lake. *Ethiopia. J. Recent Trends Biosci*, 1(1), 94–100.
- Getnet, H., Kifle, D., & Fetahi, T. (2021). Impact of water hyacinth (Eichhornia crassipes) on water quality and phytoplankton community structure in the littoral region of Koka Reservoir, Ethiopia. *International Journal of Fisheries and Aquatic Studies*, *9*(5), 266–276.
- Gilerson, A. A., Gitelson, A. A., Zhou, J., Gurlin, D., Moses, W., Ioannou, I., & Ahmed, S. A. (2010). Algorithms for remote estimation of chlorophyll-a in coastal and inland waters using red and near infrared bands. *Optics Express*, *18*(23), 24109. https://doi.org/10.1364/oe.18.024109
- Gons, H. J., Rijkeboer, M., & Ruddick, K. G. (2005). Effect of a waveband shift on chlorophyll retrieval from MERIS imagery of inland and coastal waters. *Journal of Plankton Research*, *27*(1), 125–127.

https://doi.org/10.1093/plankt/fbh151

- Haque, S. (2021). How Effective Are Existing Phosphorus Management Strategies in Mitigating Surface Water Quality Problems the U.S.?. *Sustainability*, 13, 6565. https://doi.org/10.3390/su13126565
- Hu, C. (2009). A novel ocean color index to detect floating algae in the global oceans.*Remote Sensing of Environment*, 113(2009) 2118–2129.
- Li, J., Brown, E. T., Crowe, S. A., & Katsev, S. (2018). Sediment geochemistry and contributions to carbon and nutrient cycling in a deep meromictic tropical lake: Lake Malawi (East Africa). *Journal of Great Lakes Research*, *44*(6), 1221–1234. https://doi.org/10.1016/j.jglr.2017.12.001
- Matthews, M. W., Bernard, S., & Robertson, L. (2012). An algorithm for detecting trophic status (chlorophyll-a), cyanobacterial-dominance, surface scums and floating vegetation in inland and coastal waters. *Remote Sensing of Environment*, *124*, 637–652. https://doi.org/10.1016/j.rse.2012.05.032
- Major, Y., Kifle, D., Spoof, L., & Meriluoto, J. (2018). Cyanobacteria and microcystins in Koka reservoir (Ethiopia). *Environmental Science and Pollution Research*, 25 (2018)26861–26873.
- Makwinja, R., Inagaki, Y., Sagawa, T., Obubu, J.P., Habineza, E., Haaziyu, W., 2022 Monitoring trophic status using in situ data and Sentinel-2 MSI algorithm: Lesson from Lake Malombe, Malawi, Environmental Science and Pollution Research. https://doi.org/10.1007/s11356-022-24288-8
- Mishra, S., & Mishra, D. (2012). Normalized difference chlorophyll index: A novel model for remote estimation of chlorophyll-a concentration in turbid productive waters. *Remote Sensing of Environment* , 117(2012) 394–406.
- Page, B., Kumar, A., & Mishra, D. (2018). A novel cross-satellite based assessment of the spatio-temporal development of a cyanobacterial harmful algal bloom. *International journal of applied earth observation and geoinformation*, 66 (2018) 69–81.
- Paerl, H. W. (2014). Mitigating harmful cyanobacterial blooms in a human- and climatically-impacted world.*Life*, *4*(4), 988–1012. https://doi.org/10.3390/life4040988
- Sawtell, R. W., Anderson, R., Tokars, R., Lekki, J. D., Shuchman, R. A., Bosse, K. R., & Sayers, M. J. (2019). Real time HABs mapping using NASA Glenn hyperspectral imager. *Journal of Great Lakes Research*, *45*(3), 596–608. https://doi.org/10.1016/j.jglr.2019.02.007
- Sharaf, N. (2021). Using remote sensing and modeling to monitor and understand harmful algal blooms. Application to Karaoun Reservoir (Lebanon). *Environmental Engineering*, https://pastel.archives-ouvertes.fr/tel-0340456
- Soomets, T., Uudeberg, K., Jakovels, D., Brauns, A., Zagars, M., & Kutser, T. (2020).*in Baltic Lakes Using Sentinel-2 MSI and Sentinel-3*.
- Tilahun, S., Kifle, D., Zewde, T., Johansen, J., Demissie, T., & Hansen, J. (2019). Toxicon.*Temporal dynamics of intra-and extra-cellular microcystins concentrations in Koka reservoir (Ethiopia): implications for public health risk*, 168(2019) 83–92.
- Tilahun, S., & Kifle, D. (2018). The influence of el niño-induced drought on cyanobacterial community structure in a shallow tropical reservoir (Koka reservoir, ethiopia). *Aquatic Ecology*, 53(2018) 61–77.
- Trottet, A., George, C., Drillet, G., & Lauro, F. (2021). Aquaculture in coastal urbanized areas: A comparative review of the challenges posed by Harmful Algal Blooms. *Critical Reviews in Environmental Science and Technology*, 52(16)

2888-2929. https://doi.org/10.1080/10643389.2021.1897372

- Willén, E., Ahlgren, D., Tilahun, G., Spoof, L., Neffling, M., & Meriluoto, J. (2011). Cyanotoxin production in seven Ethiopian rift valley lakes. *Inland Waters*, 1(2011) 81–91.
- Wynne, T. T., Stumpf, R. P., Tomlinson, M. C., Warner, R. A., Tester, P. A., Dyble, J., & Fahnenstiel,G. L. (2008). Relating spectral shape to cyanobacterial blooms in the Laurentian Great Lakes. *International Journal of Remote Sensing*, *29*(12), 3665–3672. https://doi.org/10.1080/01431160802007640
- Zewde, T., Johansen, J., Kifle , D., Demissie, T., Hansen, J., & Tadesse, Z. (2018). 2018. Concentrations of microcystins in the muscle and liver tissues of fish species from koka reservoir, ethiopia: A potential threat to public health. *Toxicon*, 153(2018)85–95.